Development 133, 823-832 doi:10.1242/dev.02261

Slit2 and netrin 1 act synergistically as adhesive cues to generate tubular bi-layers during ductal morphogenesis

Phyllis Strickland[1,*], Grace C. Shin[1,*], Andrew Plump[2], Marc Tessier-Lavigne[3] and Lindsay Hinck[1,†]

Development of many organs, including the mammary gland, involves ductal morphogenesis. Mammary ducts are bi-layered tubular structures comprising an outer layer of cap/myoepithelial cells (MECs) and an inner layer of luminal epithelial cells (LECs). *Slit2* is expressed by cells in both layers, with secreted SLIT2 broadly distributed throughout the epithelial compartment. By contrast, *Robo1* is expressed specifically by cap/MECs. Loss-of-function mutations in *Slit2* and *Robo1* yield similar phenotypes, characterized by disorganized end buds (EBs) reminiscent of those present in $Ntn1^{-/-}$ glands, suggesting that SLIT2 and NTN1 function in concert during mammary development. Analysis of $Slit2^{-/-}$;$Ntn1^{-/-}$ glands demonstrates an enhanced phenotype that extends through the ducts and is characterized by separated cell layers and occluded lumens. Aggregation assays show that $Slit2^{-/-}$;$Ntn1^{-/-}$ cells, in contrast to wild-type cells, do not form bi-layered organoids, a defect rescued by addition of SLIT2. NTN1 has no effect alone, but synergistically enhances this rescue. Thus, our data establish a novel role for SLIT2 as an adhesive cue, acting in parallel with NTN1 to generate cell boundaries along ducts during bi-layered tube formation.

KEY WORDS: Slit, Robo, Netrin, Neogenin, Mammary, Mouse

INTRODUCTION

Dramatic changes in shape and form occur during organogenesis as tissues are molded into three-dimensional structures. These changes involve a variety of rearrangements as cells disperse, condense or form sheets. Cells within structures project internally or externally to form protrusions, internal boundaries develop to restrict cell mixing, and canalization occurs to generate lumens. Together, these developmental processes produce the functionally coordinated array of tissues that characterize multicellular organisms.

The mammary gland undergoes an elaborate and regulated morphogenesis, establishing a tree-like epithelial structure (Silberstein, 2001). This epithelium is a bi-layered tube comprising an outer layer of MECs that ultimately contracts under the influence of hormones to squeeze milk into a central lumen from an inner layer of secretory epithelial cells (Fig. 1A). Before birth, only a simple ductal structure forms, which is transformed during puberty into a mammary tree by the process of ductal elongation, EB bifurcation and secondary branching. This morphogenesis requires the continuous addition of new cells to both layers, coordinated with the simultaneous formation of a lumen. The enlarged termini of ducts, termed EBs, are responsible for both growth and primary structure of the gland (Fig. 1A). Growth is driven by proliferation of a single layer of multi-potent progenitor cap cells at the tip of the bud, and by the underlying LECs. Cap cells differentiate into MECs, generating the outer tubular layer, and, at the same time, LECs are remodeled, generating a hollowed lumen from a relatively solid mass of cells present in the EB.

These modifications in shape and form of the gland during ductal morphogenesis require coordinated cellular interactions. In generating this double-layered structure, cells interact with each other. Proteins that may play a role in mediating these interactions are E- and P-cadherins that are expressed by the LECs and cap/MECs, respectively, and may mediate interactions between cells within a given layer (Daniel et al., 1995; Radice et al., 1997). Interactions between the cell layers, at least in the EB, are provided by the secreted cue netrin 1 (*Ntn1*), which is expressed by LECs, and binds its receptor neogenin (*Neo1*), present on the surface of cap cells (Srinivasan et al., 2003). Loss-of-function mutations in *Ntn1* and *Neo1* result in disorganized EBs, characterized by inappropriate spaces between cap and LEC layers. Significantly, this disorganization does not extend into the ducts, which appear normal (Srinivasan et al., 2003). Consequently, the identity of the adhesion system, if any, that mediates interactions between the MEC and LEC bi-layers during ductal morphogenesis is uncertain. Desmosomal constituents are present during postnatal mammary gland development, but they appear diffuse within cells and are not organized into mature junctional structures (Dulbecco et al., 1984; Nanba et al., 2001). This suggests that desmosomal components of cell adhesion are held in store and their assembly is delayed during development, perhaps allowing flexible movement of cells during tissue extension and tube formation. Later, in the mature gland, adhesion between MECs and LECs is via desmosomes that provide strong adhesion to maintain tissue architecture (Runswick et al., 2001).

SLITs, like NTNs, are well known guidance proteins, acting as cues to direct neurons and their axons to targets during neural development. Although SLITs and NTNs are structurally dissimilar, they share some of the same characteristics. They are both proteins that, although secreted, are not freely diffusible, but instead are immobilized in association with cell membranes or components of the extracellular matrix (Kappler et al., 2000; Zhang et al., 2004). Both act as bifunctional cues, capable of eliciting attractive and repulsive behaviors from cells expressing their receptors (Colamarino and Tessier-Lavigne, 1995; Englund et al., 2002; Kennedy et al., 1994; Kidd et al., 1999; Kramer et al., 2001). Furthermore, both have receptors that contain extracellular immunoglobulin domains and fibronectin type III repeats. In many proteins, these motifs act adhesively. Consequently it is not

[1]Department of Molecular, Cell and Developmental Biology University of California, Santa Cruz Santa Cruz, CA 95064, USA. [2]Merck Research Laboratories, 126 East Lincoln Avenue, Rahway, New Jersey 07065, USA. [3]Genentech, Incorporated, 1 DNA Way, South San Francisco, CA 94080, USA.

*These authors contributed equally to the work
†Author for correspondence (e-mail: hinck@biology.ucsc.edu)

Accepted 21 December 2005

surprising that, in addition to their chemotropic guidance functions, SLITs and NTNs act chemotactically at close range to positively and negatively modulate cell-cell and cell-ECM interactions (Deiner et al., 1997; Kang et al., 2004; Simpson et al., 2000; Srinivasan et al., 2003).

Here, we demonstrate a functional role for SLIT2 and its ROBO1 receptor during mammary gland morphogenesis. We show that SLIT2 is distributed throughout the epithelial compartment, whereas ROBO1 expression is restricted to cap/MECs. The analysis of glands carrying loss-of-function mutations reveals similar defects, suggesting this ligand/receptor pair function in the same pathway. *Slit2*$^{-/-}$ and *Robo1*$^{-/-}$ EBs display inappropriate spaces between the cap and LEC layers, a defect reminiscent of the phenotypes observed in outgrowths deficient for *Ntn1* and *Neo1* (Srinivasan et al., 2003). Consequently, we generated glands with homozygous deletions in both *Slit2* and *Ntn1*, and observe, in addition to defects in EB structure, a synergistic strengthening of the single-mutant phenotypes, characterized by severe ductal abnormalities that appear to stem from insufficient adhesion between MECs and LECs. In vitro assays confirm that *Slit2*$^{-/-}$; *Ntn1*$^{-/-}$ cells are severely compromised in their ability to form bi-layered organoids, and this deficiency is rescued by addition of purified SLIT2. Addition of NTN1 does not rescue on its own, but its addition with SLIT2 dramatically enhances both the number and size of bi-layered organoids generated, confirming a strong synergism between NTN1 and SLIT2. These results identify a novel, short-range function for SLIT2 as an adhesive cue acting through its ROBO1 receptor during ductal morphogenesis. Furthermore our results support a model in which dual 'axon' guidance systems (SLIT2/ROBO1 and NTN1/NEO1) mediate interactions between cells to preserve the structure of the gland during periods of rapid growth and morphogenetic modeling.

MATERIALS AND METHODS

Animals

The study conformed to guidelines set by the UCSC animal care committee (CARC). Mouse *Ntn1* severe hypomorphs, and *Slit1*, *Slit2*, *Slit3*, *Robo1* and *Robo2* nulls were generated and genotyped as described (Serafini et al., 1996; Leighton et al., 2001; Plump et al., 2002; Long et al., 2004). Double mouse mutants were generated by crossing double heterozygotes.

Transplant techniques

Mammary anlage was rescued from E16-20 embryos and transplanted into precleared fat pads of athymic nude females (Robinson et al., 2000). Tissue fragments from the resulting outgrowths were transplanted into precleared hosts to generate null and wild-type tissue controls (Srinivasan et al., 2003).

Tissue analysis

Whole gland preparations were stained for β-galactosidase activity as described (Brisken et al., 1999). Phenotypes were characterized on 6 μm longitudinal serial sections stained with anti-smooth muscle actin (SMA) and counterstained with Hematoxylin. Standard error was reported when data from multiple transplant lines were pooled in penetrance and expressivity studies.

Expression studies

The promoters for *Slit1*, *Slit3*, *Robo1* and *Robo2* drives the expression of *lacZ*. Their expression was assessed by whole gland β-galactosidase staining (Brisken et al., 1999). The *Slit2* promoter drives the expression of GFP. Expression was assessed by anti-GFP immunohistochemistry.

Immunohistochemistry

Tissue was fixed in 4% paraformaldehyde. Paraffin embedded tissue was sectioned at 6 μm and mounted serially. The following antibodies were used for analysis: anti-SMA, 1:500; anti-laminin-1, 1:50 (Sigma); anti-E-cadherin, 1:500 (BD Transduction Labs); anti-GFP, 1:50 (Molecular Probes); anti-Robo1, 1:250 (DUTT1. gift from Pamela Rabbits); and anti-SLIT2, 1:25 (SCBT). Standard protocols were followed and Vector ABC kits used for amplification.

RT-PCR of mouse mammary glands

Mammary glands from *Robo1*$^{+/+}$ 5-week-old female mice were used and total RNA was prepared using a Total RNA Purification System (Invitrogen). cDNA was made from total RNA using iScript cDNA Synthesis Kit (BioRad) and reverse-transcribed. *Robo1* and *Dutt1* specific primers were generated as described (Clark et al., 2002).

Rotary cultures

Primary mammary epithelial cells were prepared from mild collagenase and dispase digestion, as described (Darcy et al., 2000). Differential trypsinization was performed to separate MECs from LECs. These fractions were combined (4 MECs: 1 LEC) and rotated at 60 rpm at 37°C, 5% CO_2 in media at 10^6 cells/ml. SLIT2 and NTN1 were added prior to rotation. Rotary aggregates were fixed in 4% paraformaldehyde and sectioned for immunostaining (30 μm cryosections) using a MOM kit (Vector Laboratories). Aggregates were categorized based on size and whether none or one (or more) MECs were present. At least 10 aggregates were counted for each experiment.

Ductal phenotype quantification

EB arrays were embedded in paraffin and longitudinal 6 μm serial sections were immunostained for SMA to delineate the MECs layer. Slides with EBs displaying the null phenotype and with subtending ducts that could be followed in serial section were analyzed. Phenotype severity was categorized as sporadic loss of LECs if discontinuous lengths from 20-50 μm were present or as epithelial separation if lengths from 40-1000 μm of intact LECs were detached from the MEC layer. Ducts with more than one aberration were scored with the most severe phenotype.

RESULTS

Slit2 and Robo1 are expressed in the mammary gland during ductal elongation

To begin an investigation into whether SLITs and ROBOs play a role in mammary gland development, we examined the expression patterns of *Slit1*, *Slit2*, *Slit3*, *Robo1* and *Robo2*. As *Robo4* expression is reported to be specific to the vasculature (Huminiecki et al., 2002; Park et al., 2003), we did not examine this family member, nor did we pursue *Rig1*(*Robo3*) as it probably functions as a negative regulator of SLIT responsiveness rather than as a signaling receptor (Sabatier et al., 2004).

We found using immunohistochemistry that SLIT2 is broadly distributed in wild-type (+/+) tissue throughout the epithelial compartment during the period of ductal outgrowth (5 weeks). It is present in and around both cap and LECs in the EB (Fig. 1B). Little or no background immunostaining was observed in *Slit2*$^{-/-}$ outgrowths (Fig. 1C). To identify the cells that express *Slit2*, we took advantage of the expression of *GFP* under the control of the endogenous promoter in mice targeted for *Slit2* and assayed for GFP expression using immunohistochemistry. At 5 weeks of age, we observed GFP expression in *Slit2*$^{-/-}$ tissue in cap cells of the EB (Fig. 1D, arrowheads) and in LECs (Fig. 1D, arrows). Along the duct, we also observed GFP immunostaining in both MECs (Fig. 1F, arrowheads) and LECs (Fig. 1F, arrow). As this immunostaining was performed on knockout tissue, the morphological structure of the EB and duct was abnormal; these defects are described in detail in the next section. Wild-type (+/+) control tissue displays the normal EB structure, and we observed little or no background GFP staining, indicating that the detection method was specific (Fig. 1E,G). Next, we examined the expression of other *Slit* family members. We did not detect *Slit1* expression at any stage (data not shown). By contrast, taking advantage of the expression of *lacZ* under the control of the

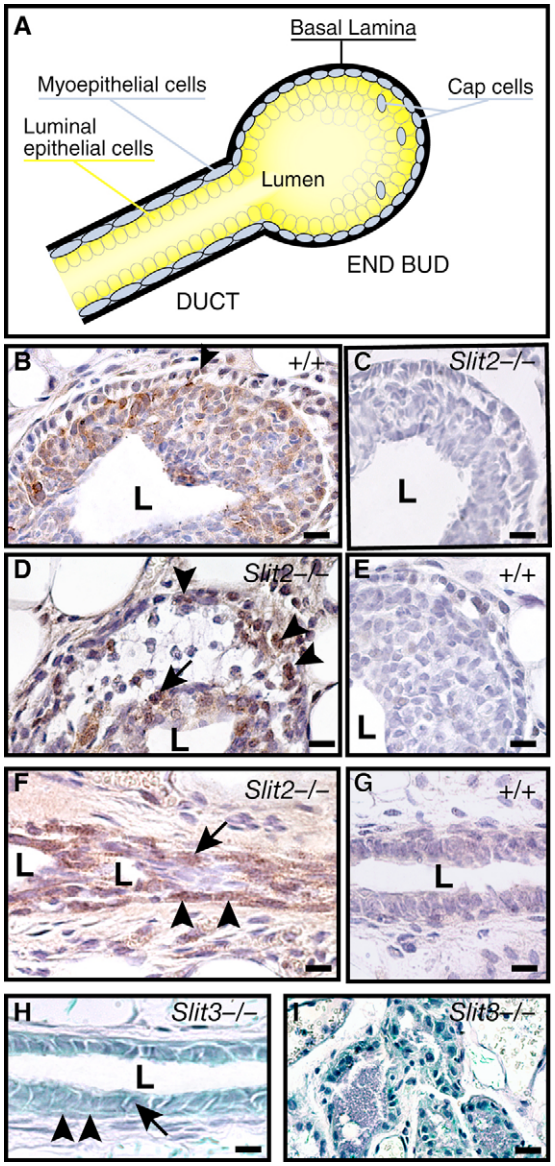

Fig. 1. Expression patterns of *Slit2* and *Slit3* during mammary gland development. (**A**) Schematic of an EB with subtending duct. (**B**,**C**) SLIT2 immunostaining on (B) +/+ and (C) *Slit2*$^{-/-}$ EBs. (**D**,**E**) GFP immunostaining on (D) *Slit2*$^{-/-}$ and (E) +/+ EBs. (**F**,**G**) GFP immunostaining on (F) *Slit2*$^{-/-}$ and (G) +/+ ducts. (H,I) *Slit3*$^{-/-}$ outgrowth stained for β-galactosidase activity. (**H**) *Slit3* expression in mature virgin duct. (**I**) *Slit3* expression in aveoli during pregnancy. Arrowheads indicate examples of positively stained cells in the cap cell layer of the EB (B,D) and in the MEC layer of the duct (F,H). Arrows indicates examples of positively stained cells in the LEC compartment of the EB (D) and duct (F,H). L, lumen. Scale bar: 20 μm.

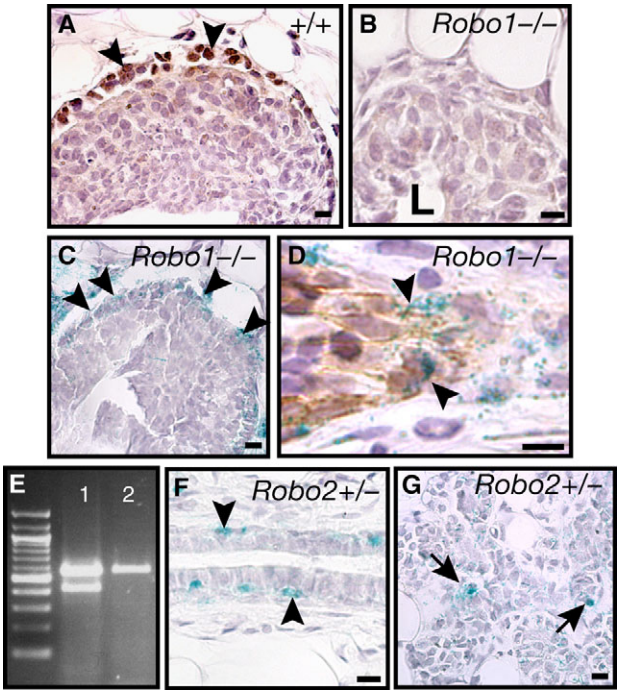

Fig. 2. Expression patterns of *Robo1* and *Robo2* during mammary gland development. (**A**,**B**) ROBO1 immunostaining on (A) $^{+/+}$ and (B) *Robo1*$^{-/-}$ EBs. (**C**,**D**) *Robo1*$^{-/-}$ outgrowth stained for β-galactosidase activity in the (C) EB and (D) duct. (D) A grazing longitudinal section through a duct. Arrowheads identify examples of MECs co-expressing *Robo1* (blue) and SMA (brown). (**E**) RT-PCR using *Dutt1*- and *Robo1*-specific primers. Lane 1, P4 cerebellum (control); lane 2, mammary gland. A 100 bp ladder (NEB) was used as a marker, as shown on the left-hand side. *Dutt1* generates a 571 bp PCR fragment and *Robo1* generates a 428 bp PCR fragment. (**F**,**G**) *Robo2*$^{+/-}$ glands stained for β-galactosidase activity in the mature virgin duct (F) and aveoli during pregnancy (G). Arrowheads indicate examples of positively stained cells in the cap cell layer of the EB (A,C) and MEC layer of the duct (D,F). (G) Arrows indicate examples of positively stained *Robo2*-expressing cells. L, lumen. Scale bar: 10 μm.

endogenous promoter in mice targeted for *Slit3*, we observed β-galactosidase staining in MECs (Fig. 1H, arrowheads) and ductal LECs (Fig. 1H, arrow) of the mature virgin *Slit3*$^{-/-}$ gland, and during pregnancy in LECs and MECs of alveoli (Fig. 1I). *Slit3*, however, was not expressed during ductal outgrowth. Moreover, no morphological defects were detected in *Slit3*$^{-/-}$ mammary glands (P.S., G.S. and L.H., unpublished), probably owing to the presence of residual SLIT2, which is expressed early and may compensate for a lack of SLIT3 later in development.

Next, we examined the expression of *Robo1* and *Robo2*, which are the receptors that mediate both the attractant and repellent effects of SLIT proteins. Immunohistochemical analysis on wild-type (+/+) tissue demonstrated ROBO1 expression specifically on cap cells in the EB (Fig. 2A) and MECs of the duct (data not shown), with little or no background immunostaining observed in *Robo1*$^{-/-}$ tissue (Fig. 2B). Once again, we took advantage of the expression of *lacZ* under the control of the endogenous *Robo1* promoter in $^{-/-}$ and $^{-/+}$ tissue to confirm our immunohistochemical results. We observed β-galactosidase staining specifically in cap cells of the EB (Fig. 2C, arrowheads) and MECs in the duct where it co-localized with the marker smooth muscle actin (SMA) (Fig. 2D). As the expression of two isoforms of *Robo1* has been reported during mouse development (Clark et al., 2002), we determined that the *Dutt1* isoform is specifically expressed in the developing mammary gland by performing RT-PCR analysis on mRNA (Fig. 2E). We also examined *Robo2* expression by staining *Robo2*$^{+/-}$ tissue, and, similar to *Slit3*, found it was not expressed during ductal outgrowth (data not shown), but was expressed later in development in a subset of ductal MECs in the mature virgin animal (Fig. 2F, arrowheads) and during pregnancy in alveoli (Fig. 2G, arrows).

Loss of either *Slit2* or *Robo1* results in abnormal EBs that are morphologically similar to *Ntn1*$^{-/-}$ and *Neo1*$^{-/-}$ EBs

To investigate the role of SLIT proteins in mammary gland development, we analyzed glands carrying loss-of-function alleles of *Slit2* and *Robo1*. The perinatal lethality of the *Slit2*$^{-/-}$ mutation prevented the study of mammary glands in mice carrying the homozygous mutation. Consequently, we followed standard protocols and harvested mammary anlage from *Slit2*$^{-/-}$ embryos and transplanted the tissue into fat pads of immunocompromised mice that had been cleared of their epithelial tissue (Robinson et al., 2000; Young, 2000). In all studies, littermate control $^{+/+}$ outgrowths were generated on the contralateral side for comparison, ensuring that the $^{+/+}$ and $^{-/-}$ outgrowths were subjected to the same systemic environment.

We sectioned *Slit2*$^{-/-}$ outgrowths 2-3 weeks post-transplantation to analyze EBs as whole-mount analysis revealed no obvious morphological defects (data not shown). The sections were stained with an SMA antibody to visualize cap and MECs (Fig. 3A-G). Compared with an EB from control outgrowths (Fig. 3A), which displayed close apposition of the cap and LEC layers, *Slit2*$^{-/-}$ EBs displayed severe abnormalities. In *Slit2*$^{-/-}$ EBs, there were significant gaps between the LECs and cap cells, creating exaggerated subcapsular spaces, ranging from 40-50 μm compared with the 0.1-1 μm space typically observed in $^{+/+}$ EBs (Fig. 3, compare A and B). Frequently, there were dissociated cells present in this space and immunostaining with anti-SMA identified these as cap cells (Fig. 3B). The appearance of shrunken nuclei in many of these detached cells suggested that they were apoptotic and probably dying by anoikis, similar to the detached cells present in *Ntn1*$^{-/-}$ glands (Srinivasan et al., 2003). In some EBs, we observed regions where LECs were completely detached from cap cells, leaving an intact cap cell layer devoid of underlying LECs (Fig. 3C, between arrows). These single layers of cap cells commonly folded inwards, resulting in double-layered invaginations that disorganized the underlying LECs and occluded the inner luminal space (Fig. 3D, between arrowheads). The phenotype was 100% penetrant with ~60% of the EBs in every outgrowth affected (59.1±26.5%, n=98 EBs, 12 outgrowths).

A similar analysis was performed on *Robo1*$^{-/-}$ glands. As mice carrying the *Robo1* mutation were viable, intact glands were examined, although we confirmed that a similar phenotype was present when *Robo1*$^{-/-}$ tissue was transplanted (data not shown). For these experiments, glands from $^{+/+}$ littermates served as control tissue. EBs in *Robo1*$^{-/-}$ glands were disorganized, displaying a phenotype that was indistinguishable from the phenotype displayed in *Slit2*$^{-/-}$ EBs, characterized by subcapsular spaces, invaginated cap cell layers and disorganized LECs (Fig. 3F,G). As is the case for *Slit2*$^{-/-}$ outgrowths, the penetrance of the phenotype was 100% with ~60% of the EBs in every EB array affected (62±23%, n=74 EBs, four outgrowths).

A noteworthy aspect of the defects observed in *Slit2*$^{-/-}$ and *Robo1*$^{-/-}$ EBs was their striking similarity to the defects observed in *Ntn*$^{-/-}$ and *Neo1*$^{-/-}$ EBs (Srinivasan et al., 2003). One major similarity was that EBs from each homozygous null animal exhibited loss of adhesion between the LEC and cap layers, with dissociated cap cells present in the resulting subcapsular space (Fig. 3B,F). These shared defects created the impression that *Ntn1*$^{-/-}$, *Neo1*$^{-/-}$, *Slit2*$^{-/-}$ and *Robo1*$^{-/-}$ phenotypes were identical, but we detected at least one unique characteristic in *Slit2*$^{-/-}$ and *Robo1*$^{-/-}$ EBs. The cap cell layer of *Slit2*$^{-/-}$ and *Robo1*$^{-/-}$ EBs folded into the LEC compartment (Fig. 3D,G), and this was never observed in *Ntn1*$^{-/-}$ and *Neo1*$^{-/-}$ glands (Srinivasan et al., 2003). Despite this difference, the overall appearance of EBs from each knock-out suggested the defects were due to a general loss of cell-cell adhesion between cap and LEC layers (Srinivasan et al., 2003). EBs are highly proliferative structures that undergo active remodeling and are consequently more likely to be sensitive to impaired cell adhesion. As we discovered disorganization in this sensitive structure when either NTN/NEO or SLIT2/ROBO1 signaling system was lost, we expect, if these guidance systems functionally compensate for one another, that loss of both systems simultaneously will lead to disrupted cell contacts in more stable regions of the gland that are insensitive to the loss of either system alone.

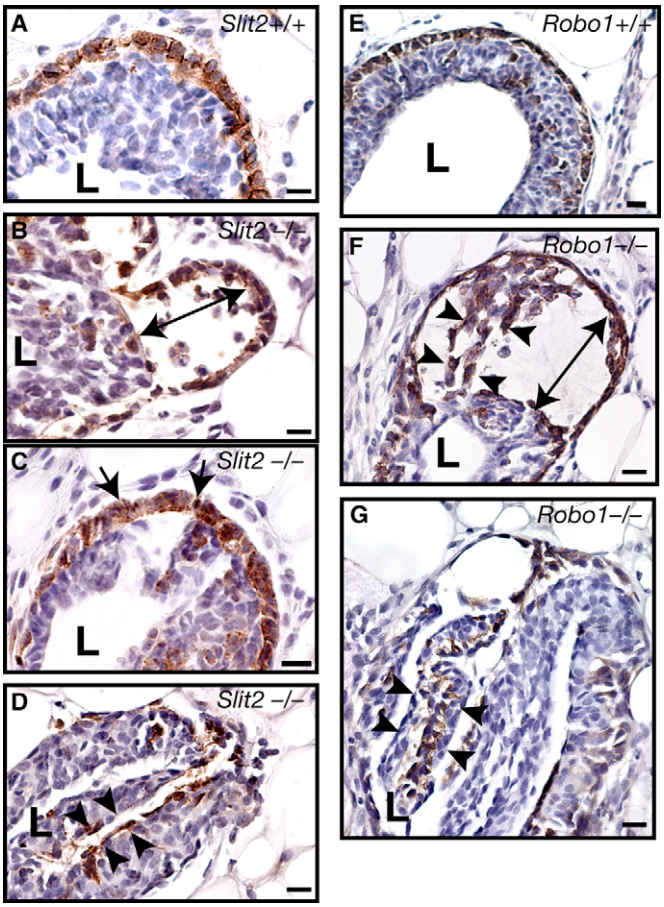

Fig. 3. Loss of either *Slit2* or *Robo1* leads to similarly abnormal EBs. (A-G) EBs immunostained with an antibody directed against SMA to identify cap cell layers. (**A**,**E**) Wild-type (+/+) EB morphology shows tight juxtaposition of cap and LEC layers. (**B-D**) Longitudinal sections through *Slit2*$^{-/-}$ EBs. (B) Exaggerated space between the cap and LEC layers (double arrowhead), and dissociated cells detected in subcapsular space. (C) Loss of LECs underlying the cap cell layer (between arrows). (D) Complete disruption of EB morphology characterized by the infolding of cap cells into the LEC compartment (arrowheads) leading to lumen loss. (**F**,**G**) Longitudinal sections through *Robo1*$^{-/-}$ EBs. (F) Exaggerated space between the cap and LEC layers (double arrowheads), dissociated cells in the subscapular space and infolding of the cap cell layer into the LEC compartment (arrowheads). (G) Complete disruption of EB morphology characterized by the infolding of cap cells into the LEC compartment (arrowheads) leading to lumen loss. (A-D) *Slit2*$^{-/-}$ outgrowths were generated by transplantation with contralateral $^{+/+}$ control outgrowths. (E-G) *Robo1*$^{-/-}$ and $^{+/+}$ mammary glands were from littermates. L, lumen. Scale bar: 20 μm.

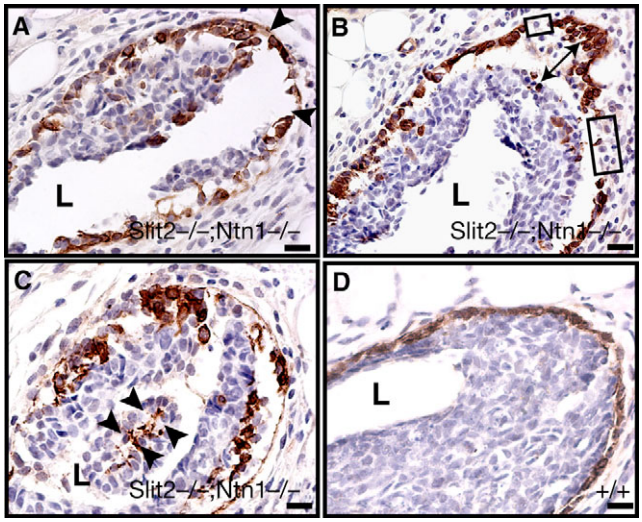

Fig. 4. Combined loss of *Slit2* and *Ntn1* leads to abnormal EB morphology with characteristics of both *Slit2*$^{-/-}$and *Ntn1*$^{-/-}$ EBs. All EBs immunostained with antibody generated against SMA. (A-C) *Slit2*$^{-/-}$;*Ntn1*$^{-/-}$ EBs. (**A**) Loss of LECs underlying the cap cell layer (between arrowheads). (**B**) Separation of the cap cell layer from the LEC layer (double arrowhead) and breaks in the basal lamina (rectangles). (**C**) Complete disruption of EB morphology characterized by the infolding of cap cells into the LEC compartment (arrowhead) leading to lumen loss. (**D**) $^{+/+}$ EB. L, lumen. Scale bar: 20 μm.

Loss of Both *Slit2* and *Ntn1* results in disrupted ductal structure in addition to abnormal EBs

To investigate whether SLIT2 and NTN1 function in parallel to maintain interactions between the cap/MEC and LEC layers during mammary gland development, we generated double homozygous null outgrowths. To analyze EBs, we sectioned *Slit2*$^{-/-}$;*Ntn1*$^{-/-}$ outgrowths 2-3 weeks post-implantation and immunostained with SMA antibody to visualize cap cells. The EBs displayed abnormalities with combined characteristics of both *Ntn1*$^{-/-}$ and *Slit2*$^{-/-}$ outgrowths (Fig. 4). Consequently, in addition to the subcapsular space and dissociated cells typically exhibited in outgrowths harboring homozygous loss-of-function alleles at either gene locus (Fig. 4B), we observed cap cell layers devoid of underlying LECs (Fig. 4A, between arrowheads) and cap cell layer enfolding (Fig. 4C, between arrowheads), both characteristic of defects observed in *Slit2*$^{-/-}$ outgrowths (Fig. 3C,D). Moreover, we also observed regions where the cap cell layer appeared completely disrupted (Fig. 4B, box), a defect exhibited in *Ntn1*$^{-/-}$ outgrowths (Srinivasan et al., 2003) but not in *Slit2*$^{-/-}$ and *Robo1*$^{-/-}$ EBs. As cap cells make and secrete the basal lamina, the loss of their integrity in the *Slit2*$^{-/-}$;*Ntn1*$^{-/-}$ EBs may destabilize the laminin network surrounding the EB as it does in the *Ntn1*$^{-/-}$ EBs (Srinivasan et al., 2003). To examine this possibility, we immunostained *Slit2*$^{-/-}$, *Robo1*$^{-/-}$ and *Slit2*$^{-/-}$;*Ntn1*$^{-/-}$ outgrowths with laminin 1 antibody (Fig. 5), the major laminin in the basal lamina (Klinowska et al., 1999). As expected, there were clear breaks in the basal lamina in the *Slit2*$^{-/-}$;*Ntn1*$^{-/-}$ EBs (Fig. 5E) (Srinivasan et al., 2003), whereas the basal lamina in the *Slit2*$^{-/-}$ and *Robo1*$^{-/-}$ EBs was intact (Fig. 5A,C). The phenotype observed in *Slit2*$^{-/-}$;*Ntn1*$^{-/-}$ outgrowths was 100% penetrant with ~80% of the EBs affected (82.6±15.4% n=103 EBs, eight outgrowths). This represented an ~20% increase in expressivity compared with the expressivity exhibited in *Slit2*$^{-/-}$ EBs (Fig. 3) or *Ntn1*$^{-/-}$ EBs (Srinivasan et al., 2003). Together with the observation that the *Slit2*$^{-/-}$;*Ntn1*$^{-/-}$ phenotype was more severe in EBs (Fig. 4) and ducts (see below) compared with the phenotype exhibited in outgrowths carrying single homozygous null alleles, our analysis suggests that NTN/NEO and SLIT/ROBO pathways function in parallel to mediate contacts between epithelial cell layers.

In addition to abnormal EBs, the ducts of *Slit2*$^{-/-}$;*Ntn1*$^{-/-}$ glands displayed severe adhesion defects. Compared with the ductal structure displayed in $^{+/+}$ tissue, which illustrates the typically close apposition between LEC and MEC layers (Fig. 6D), SMA immunostaining of double homozygous deficient outgrowths showed significant loss of adhesion between these layers (Fig. 6A,B). In the mildest form, a few LECs were sporadically detached from the MEC layer (Fig. 6A, arrows). A more severe defect was observed when this modest detachment of cells expanded to encompass substantial lengths of the duct, with the LEC layer essentially peeled away from the MEC layer (Fig. 6B, double arrowheads). Interestingly, the MECs (Fig. 6) and basal lamina (Fig. 5B,D,F) along the ducts were intact in *Slit2*$^{-/-}$;*Ntn1*$^{-/-}$ and in *Slit2*$^{-/-}$ and *Robo1*$^{-/-}$ ducts, suggesting that loss of adhesion occurs within the duct, affecting the adhesion between MEC and LEC layers. The contralateral control glands never displayed abnormal tissue morphology.

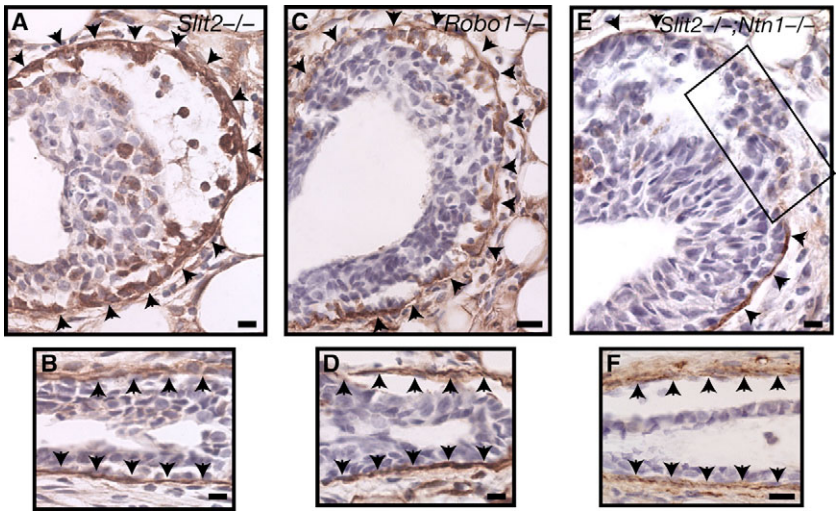

Fig. 5. The basal lamina is disrupted surrounding *Slit2*$^{-/-}$;*Ntn1*$^{-/-}$ EBs, but it is intact surrounding *Slit2*$^{-/-}$ and *Robo1*$^{-/-}$ EBs and all ducts. Immunostaining with anti-laminin 1 on EBs (A,C,E) and ducts (B,D,F). (**A**,**B**) *Slit2*$^{-/-}$ EB and duct. (**C**,**D**) *Robo1*$^{-/-}$ EB and duct. (**E**,**F**) *Slit2*$^{-/-}$;*Ntn1*$^{-/-}$ EB and duct. Arrowheads indicate regions of intact basal lamina. Boxed region (E) indicates area where the basal lamina is disrupted. Scale bar: 20 μm.

We categorized the ductal phenotype as mild (+, sporadic loss of LECs) and more severe (++, separation of myoepithelial and LEC layers) (Fig. 6C). The ducts were characterized by identifying abnormal EBs and then, when longitudinal sections allowed, tracing the subtending duct back for up to 2 mm. Although we never observed ductal abnormalities in *Ntn1*$^{-/-}$ outgrowths, ductal abnormalities were readily apparent in *Slit2*$^{-/-}$ (n=12) and double *Slit2*$^{-/-}$;*Ntn1*$^{-/-}$ (n=18) outgrowths (compare Fig. 6G with 6A,B,E). The loss of *Slit2* resulted in both sporadic LEC loss (50%) and separation of the epithelial cell layers (50%). By contrast, the more severe phenotype of epithelial separation was the major phenotype present (89%) in the absence of both *Slit2* and *Ntn1*. Taken together, the data showed that loss of either *Slit2*$^{-/-}$ or *Ntn1*$^{-/-}$ results in cell-cell adhesion defects between cap and LEC layers in the EB (Fig. 3) (Srinivasan et al., 2003). This loss in adhesion extends into the duct in *Slit2*$^{-/-}$, but not *Ntn1*$^{-/-}$, outgrowths (Fig. 6E,G). The subtle role for NTN1 in ductal morphogenesis is only revealed by the additional removal of *Ntn1* in a *Slit2*$^{-/-}$ background which increases the severity of the ductal defects (Fig. 6A,B). This suggests that, while SLIT2 plays a primary role in mediating interactions between LEC and MEC layers during ductal morphogenesis, NTN1 synergistically contributes to these interactions.

SLIT2 and NTN1 mediate contacts between LEC and MEC layers

In the nervous system, studies have shown that SLIT/ROBO signaling inactivates N-cadherin-mediated adhesion (Rhee et al., 2002). As we observe adhesive defects predominantly in the LEC compartment of *Slit2*$^{-/-}$;*Ntn1*$^{-/-}$ outgrowths where E-cadherin has been shown to mediate interactions (Daniel et al., 1995), we performed immunohistochemistry using anti-E-cadherin. We observed, as expected, robust membrane staining around LECs on $^{+/+}$ control glands. We also observed similar robust immunostaining between LECs of *Slit2*$^{-/-}$;*Ntn1*$^{-/-}$ EBs and ducts (see Fig. S1A-D in the supplementary material), indicating that cadherin-mediated contacts are not altered in double homozygous null tissue.

Next, we focused on proteins that mediate the interaction between LEC and MEC layers. Although desmosomal components mediate these contacts in mature ducts (Runswick et al., 2001), they are not assembled during branching morphogenesis (Dulbecco et al., 1984; Nanba et al., 2001). Consequently, we entertained the possibility that contact between layers was mediated, either directly or indirectly, by SLIT2 and NTN1. We investigated by using an in vitro aggregation assay to examine whether primary cells, harvested from *Slit2*$^{-/-}$;*Ntn1*$^{-/-}$ outgrowths, were impaired in their ability to generate bi-layered epithelial structures. Previous studies have shown that mixtures of wild-type, primary mammary cells form aggregates of LECs surrounded by single layers of MECs (Runswick et al., 2001). This appears to be a timed aggregation with LECs forming clusters that MECs attach to and surround. In agreement with the previous study, we confirmed that wild-type mammary cells form bi-layered organoids (Fig. 7A).

Next, we generated aggregates from *Slit2*$^{-/-}$;*Ntn1*$^{-/-}$ cells and observed that, although LEC aggregates formed, few were surrounded by MECs. To quantify this assay, we considered a structure bi-layered with one or more MECs surrounding the LEC aggregate. Even with this lenient definition, we found that 70% of *Slit2*$^{-/-}$;*Ntn1*$^{-/-}$ aggregates lacked a bi-layer (Fig. 7B). Of the 30% *Slit2*$^{-/-}$;*Ntn1*$^{-/-}$ aggregates categorized as having a bi-layer, many contained just one or only a few MECs on the outer surface, compared with $^{+/+}$ aggregates, which generally displayed fully formed MEC layers (Fig. 7A). A second characteristic of *Slit2*$^{-/-}$;*Ntn1*$^{-/-}$ aggregates was that they appeared smaller than wild-type aggregates. To quantify aggregate size, we counted the number of cells comprising each and categorized them as: fewer than 10 cells, between 10 and 20 cells, and greater than 20 cells (Fig. 7K). All wild-type organoids contained greater than 10 cells and the majority contained greater than 20. By contrast, the majority of

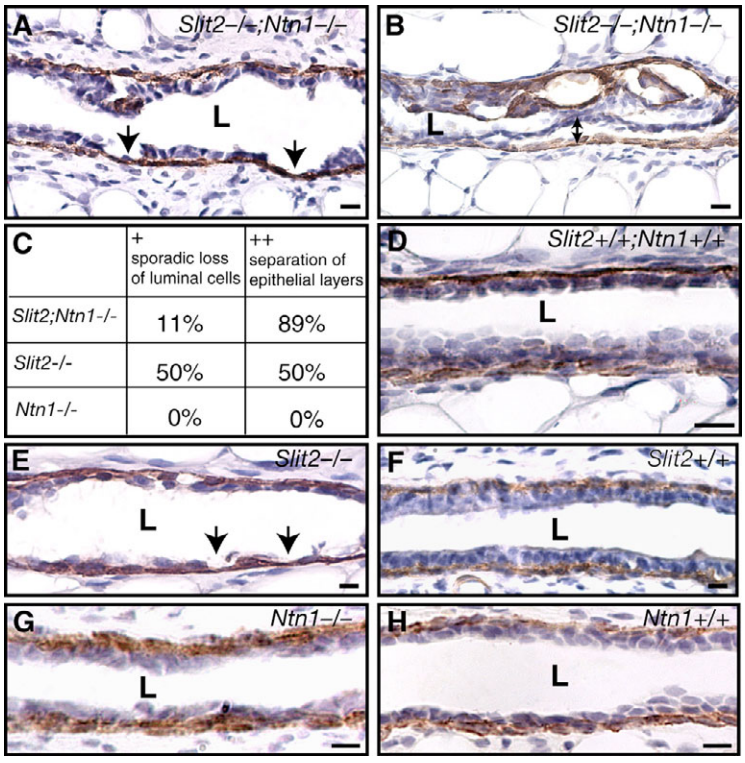

Fig. 6. Loss of both *Slit2* and *Ntn1* and leads to separation of epithelial cell layers in the duct. All ducts are immunostained with antibody generated against SMA. (A,B) *Slit2*$^{-/-}$;*Ntn1*$^{-/-}$ ducts. (**A**) Moderate disruption characterized by sporadic loss of LECs (arrows). (**B**) Separation of epithelial layer (double arrowhead). (**C**) Table quantifying the severity of ductal disruption. *Ntn1*$^{-/-}$ ducts are normal, whereas *Slit2*$^{-/-}$ and *Slit2*$^{-/-}$;*Ntn1*$^{-/-}$ ducts display increasingly severe disorganization. (+) Modest disruption is characterized by sporadic loss of LECs in short (~50 μm) length of duct. (++) More severe disruption is characterized by significant stretches (~50-2000 μm) of separation of myoepithelial and LEC layers. (**D**) *Slit2*$^{+/+}$;*Ntn1*$^{+/+}$ duct from contralateral transplant shows tight juxtaposition of myoepithelial and LEC layers, and an unobstructed lumen. (**E**,**F**) Loss of *Slit2* (E) leads to sporadic loss of LECs (arrows) in the duct, compared with *Slit2*$^{+/+}$ duct (F) from contralateral transplant duct. (**G**,**H**) *Ntn1*$^{-/-}$ duct (G) appears morphologically indistinguishable compared with *Ntn1*$^{-/-\ +/+}$ duct (H) from contralateral transplant. L, lumen. Scale bar: 20 μm.

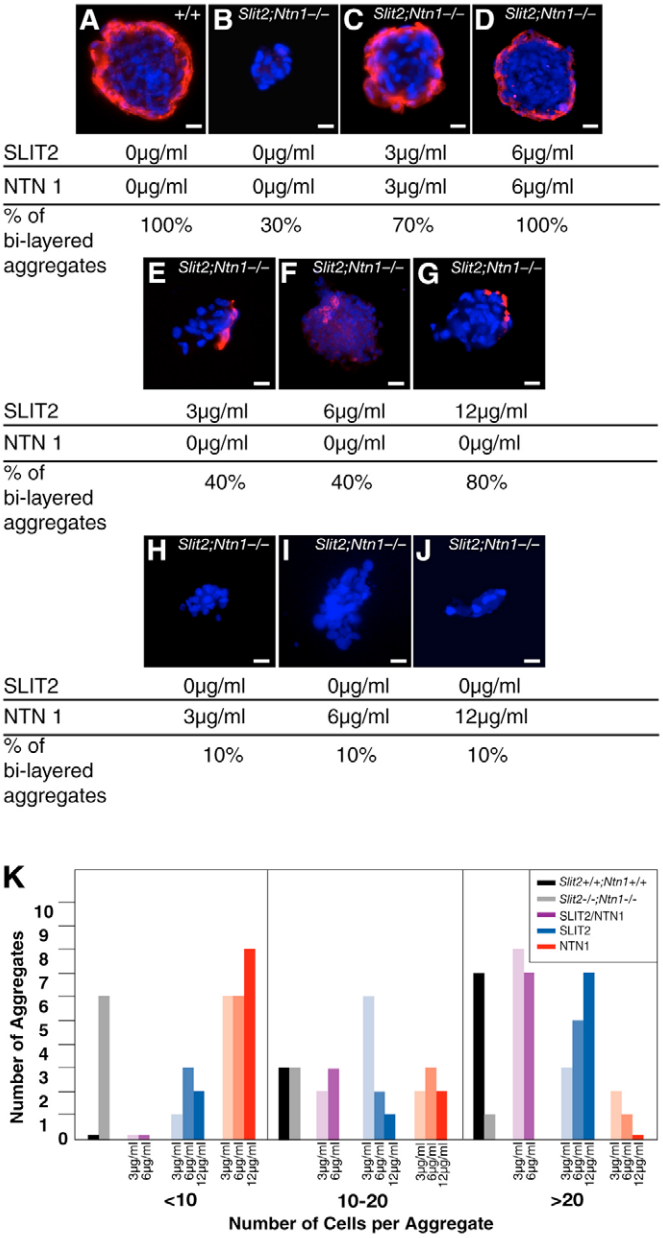

Fig. 7. *Slit2*$^{-/-}$;*Ntn1*$^{-/-}$ MECs are unable to form bi-layered aggregates in vitro. (A-J) Aggregates are stained with SMA (red) and DAPI (blue). Bi-layered is defined as having one or more MECs surrounding the LEC aggregate. (**A**) Wild-type aggregates are bi-layered, with MECs surrounding an LEC aggregate. (**B**) Thirty percent of *Slit2*$^{-/-}$;*Ntn1*$^{-/-}$ aggregates are bi-layered compared with wild type. Addition of (**C**) 3 μg/ml or (**D**) 6 μg/ml of SLIT2 and NTN1 restores bi-layered structure of the aggregates. Addition of (**E**) 3 μg/ml, (**F**) 6 μg/ml or (**G**) 12 μg/ml SLIT2 alone partially restores bi-layered aggregate structure. Bi-layered aggregation is not restored in the presence of (**H**) 3 μg/ml, (**I**) 6 μg/ml or (**J**) 12 μg/ml NTN1 alone. Quantification of percentage bi-layered aggregation is below each representative aggregate picture. (**K**) Quantification of aggregate size in the absence or presence of SLIT2 and NTN1. *Slit2*$^{-/-}$;*Ntn1*$^{-/-}$ cells (gray) form greater numbers of smaller aggregates compared with wild-type cells (black). In the presence of 3 μg/ml or 6 μg/ml of SLIT2 and NTN1, *Slit2*$^{-/-}$;*Ntn1*$^{-/-}$ cells form larger aggregates (purple). They also form larger aggregates in the presence of SLIT2 alone (blue), but with NTN1 alone (orange), the aggregates remain small. Scale bar: 10 μm.

aggregates composed of *Slit2*$^{-/-}$;*Ntn1*$^{-/-}$ cells was small (<10 cells), consistent with a role for the MEC layer, which does not form when *Slit2*$^{-/-}$;*Ntn1*$^{-/-}$ aggregate, in stabilizing clustered LECs in rotary culture. We never observed MECs inappropriately mixed into LEC aggregates, a situation that occurs when desmosomal adhesion in disrupted (Runswick et al., 2001). Thus, although *Slit2*$^{-/-}$;*Ntn1*$^{-/-}$ LECs aggregated properly, *Slit2*$^{-/-}$;*Ntn1*$^{-/-}$ MECs were severely deficient in their ability to adhere to the outside of LEC aggregates even though they express ROBO1 and NEO1 (Fig. 2) (Srinivasan et al., 2003).

To confirm this deficiency is due to the lack of SLIT2 and NTN1, we repeated the experiment in the presence of 3 μg/ml and 6 μg/ml of SLIT2 and NTN1. With 3 μg/ml of each protein, the percent of aggregates forming bi-layered structures increased from 30% to 70%, with the majority of organoids exhibiting fully formed myoepithelial layers (Fig. 7C). With 6 μg/ml of each protein, bi-layered aggregation was fully rescued (Fig. 7D). To evaluate whether SLIT2 or NTN1 alone were sufficient to rescue the phenotype, we performed the rescue experiment with 3 μg/ml, 6 μg/ml or 12 μg/ml of each protein alone. At 3 μg/ml and 6 μg/ml of SLIT2, 40% of the *Slit2*$^{-/-}$;*Ntn1*$^{-/-}$ aggregates formed bi-layered structures, at 12 μg/ml this number increased to 80% (Fig. 7E-G). Although these organoids were relatively large with the majority composed of greater than 10 cells (Fig. 7K), they lacked the fully formed MEC layers that were observed when the rescue experiment was performed with both SLIT2 and NTN1 (Fig. 7, compare C,D with E-G). Addition of NTN1 alone yielded only small aggregates with just 10% considered bi-layered because one or two MECs clung to the outer perimeter (Fig. 7H-J). Interestingly, this 10% bi-layered aggregation in the presence of NTN1 was less than the 30% bi-layered aggregation observed under control conditions in the absence of NTN1 and SLIT2, suggesting that NTN1 alone had a modest inhibitory effect on aggregation. Taken together, the data suggest that SLIT2, acting through ROBO1 expressed on MECs (Fig. 2), mediates contacts between LECs and MECs. This contact formation is enhanced in the presence of NTN1 whose receptor, NEO1, is also specifically expressed on MECs (Srinivasan et al., 2003). At 3 μg/ml and 6 μg/ml of SLIT2, 40% of the aggregates were bi-layered, a number that increased to 70% and 100%, respectively, with the addition of NTN1 (Fig. 7C-F). The observation that NTN1 acts in concert with SLIT2 to rescue bi-layered aggregation in vitro is consistent with the phenotypes observed in vivo. A ductal phenotype is observed in *Slit2*$^{-/-}$, but not *Ntn1*$^{-/-}$ outgrowths, and the defects are synergistically strengthened by the additional loss of *Ntn1* in a *Slit2*$^{-/-}$ background (Fig. 5). Thus, SLIT2 and NTN1 function in concert during mammary ductal morphogenesis to generate tubular bi-layers by mediating interactions between distinct epithelial layers.

DISCUSSION

During development, bi-layered ducts of mammary epithelium are generated as EBs invade the fat pad forming an elaborately branched structure. Taking advantage of the relatively simple model system of mammary ductal development, we examined the role of two different families of 'axon guidance' cues during epithelial morphogenesis. Using both in vivo and in vitro approaches, we provide evidence that SLIT2 and NTN1 act synergistically to generate adhesive contacts between the epithelial layers comprising a tubular bi-layer. Our data support a model in which these cues work in parallel at short range as adhesive cues to maintain tissue structure while allowing cell movement and re-organization during periods of rapid tissue growth and remodeling.

Members of functionally-related families act synergistically during mammary ductal morphogenesis

During mammary ductal development, only the *Slit2* and *Robo1* members of these gene families are expressed in the gland. Although secreted SLIT2 protein is widely distributed throughout the epithelial compartment, ROBO1 is expressed specifically by cap and MECs (Figs 1, 2). Glands harboring loss-of-function mutations in either gene exhibit similar phenotypes, strongly supporting a model in which SLIT2 signals through ROBO1 at this stage of development. Defects in *Slit2*$^{-/-}$ and *Robo1*$^{-/-}$ glands are confined to the EB and, although relatively modest, are consistent with the loss of stabilizing interactions (Fig. 3). *Slit2*$^{-/-}$ and *Robo1*$^{-/-}$ EBs exhibit a general disorganization in cell contacts with inappropriate spaces forming between the cap and LEC layers. Dissociated cells fill these subcapsular spaces and layers of cap cells fold inwards, occluding lumenal space. Taken together, these results suggest that SLIT2-mediated activation of ROBO1 is required to maintain the proper positioning of cap and LEC layers in the EB.

Our previous studies have already implicated the NTN/NEO guidance system in maintaining proper positioning of cap cells at the leading edge of the EB (Srinivasan et al., 2003). We proposed that NTN1, expressed by LECs, acts adhesively as a short-range attractant to maintain the position of NEO1-expressing cap cells. The similarity in the defects exhibited by *Ntn1*$^{-/-}$ and *Slit2*$^{-/-}$ EBs prompted us to investigate the consequences of genetically interrupting the expression of genes encoding both guidance cues. We show that loss of *Ntn1* in a *Slit2*$^{-/-}$ background results in synergistic strengthening of the single-mutant phenotypes (Figs 4-6). Moreover addition of NTN1 synergistically enhances the ability of SLIT2 to rescue bi-layered aggregation of *Slit2*$^{-/-}$;*Ntn1*$^{-/-}$ mammary cells (Fig. 7). Our results are consistent with a model in which two different guidance systems act in parallel to mediate interactions between distinct epithelial cell types during organ development, although we have not excluded the possibility that some crossregulation between these systems occurs (Stein and Tessier-Lavigne, 2001).

SLIT2 signals through ROBO1 as a short-range adhesive cue

Our experiments support a positive role for SLIT2 in the developing gland. First, the loss of cell-cell interactions observed in *Slit2*$^{-/-}$ and *Robo1*$^{-/-}$ EBs is consistent with the loss of a stabilizing interaction (Fig. 3). Second, we observed that simple addition of purified SLIT2 rescues the ability of *Slit2*$^{-/-}$;*Ntn1*$^{-/-}$ cells to form bi-layered organoids (with NTN1 contributing synergistically). As SLIT2 is not presented in a way that provides directional information, its role in the gland appears to be adhesive, which is different from the guidance role that SLITs play in the nervous system (Fig. 7). This type of short-range adhesive role has already been proposed for NTN1 and NEO1 (Srinivasan et al., 2003). At least two models that are not mutually exclusive can be proposed for the mechanism by which SLIT2/ROBO1 (and NTN1/NEO1) mediate cell-cell adhesion between epithelial cell layers. One model is that SLIT2 acts directly as an adhesive factor, binding ROBO-expressing cap/MECs and stabilizing the interaction between these two layers. As SLIT2 is secreted (Fig. 1F), this model requires that it associates with LECs. Association probably occurs via heparin sulfate proteoglycans that have been shown to bind, concentrate and stabilize SLITs (Ronca et al., 2001; Steigemann et al., 2004). Candidate proteoglycans on LECs are glypican and syndecan (Delehedde et al., 2001), but there may also be a requirement for proteoglycans on receptor expressing MECs as genetic studies in *Drosophila* have shown that syndecan serves as a necessary co-receptor for ROBO in transducing the SLIT signal (Steigemann et al., 2004).

The second model is that SLIT2 signals through ROBO1 to affect cell adhesion indirectly by modulating the expression or function of other cell adhesion proteins. A candidate cell adhesion protein that could be the target of SLIT/ROBO signaling is Ep-CAM, which mediates Ca^{2+} independent, homotypic cell-cell adhesion (Balzar et al., 1999a; Balzar et al., 1999b). One problem with this candidate is that Ep-CAM, like E-cadherin (see Fig. S1 in the supplementary material), mediates adhesion between individual LECs and not between LEC and MECs, the contacts of which appear disrupted in *Slit2*$^{-/-}$;*Ntn1*$^{-/-}$ glands. Candidates that mediate interactions between LEC and MECs, such as desmoglein or desmocollin, function in the mature gland (Runswick et al., 2001), and although they are present in the developing gland, they have not yet formed adhesive junctional complexes (Dulbecco et al., 1984; Nanba et al., 2001). Consequently, we favor the first model in which SLIT2 and ROBO1 act directly as cell-adhesion proteins, but currently our data do not rule out the second model. To distinguish between these two models, we are currently investigating the signaling events downstream of SLIT2/ROBO1 and NTN1/NEO1.

Most studies on SLIT/ROBO signaling have focused on its inhibitory and chemorepulsive influence on cell migration and axon guidance, although there are a few examples that demonstrate the outgrowth promoting and chemoattractive activities of SLIT. For example, human vascular endothelial cells are attracted to SLIT-expressing tumors (Wang et al., 2003), and *Drosophila* mesodermal cells are attracted to SLIT-expressing muscle attachment sites (Kramer et al., 2001). SLITs are also positive regulators of elongation and branch formation for both rat sensory neurons and *Drosophila* tracheal cells (Englund et al., 2002; Wang et al., 1999). Although none of these studies demonstrate SLIT acting to increase cell-cell interactions at short range, the process of guidance at long-range must involve a series of local interactions as cells or axons move up a gradient towards the source of cue. Similarly processes such as branch formation must involve local interactions as a restricted portion of the target membrane preferentially protrudes and becomes stabilized. In the mammary gland, our data suggest that SLIT2, which is secreted by target cells, is available on cell surfaces in the epithelium where it interacts with ROBO1 present on the surface of cap/MECs. Their interaction maintains tissue architecture and restricts inappropriate intermingling by mediating contacts between distinct epithelial cells layers.

These examples establish positive roles for SLITs and ROBOs in cell migration, branch formation and interepithelial interactions, but studies on the repellent activity of SLITs have supplied details concerning the mechanisms by which the SLIT/ROBO signal is transduced. The intracellular domain of ROBO1 contains four motifs that have been shown to interact with a number of signaling proteins, including the actin binding protein ENABLED (murine MENA) (Bashaw et al., 2000; Yu et al., 2002), the nonreceptor Abelson tyrosine kinase, c-ABL (Bashaw et al., 2000), the adaptor DOCK (Fan et al., 2003) and the GTPase-activating protein srGAP1 (Wong et al., 2001). All these signaling proteins are candidates for mediating the attractive and adhesive activities of ROBO. Indeed, before their roles as negative regulators of ROBO signaling were revealed, DOCK was identified as a positive regulator in axon outgrowth and synapse formation (Desai et al., 1999; Garrity et al., 1996), and MENA was shown to promote actin dependent motility (Krause et al., 2002). All these signaling proteins are also candidates for mediating the interaction of ROBO1 with the cytoskeleton, leading to changes in the mobility or adhesiveness of cells.

Concluding remarks

Our discovery that members of functionally related families act in similar ways during development suggests an explanation for the observation that single loss-of-function mutations and even multiple loss-of-function mutations in family members of genes encoding 'axon guidance' cues have failed to yield phenotypes in many vertebrate organ systems. For example, lungs of embryos carrying loss-of-function alleles in both *Ntn1* and *Ntn4* display no apparent phenotype, even though treatment of lung explants in vitro with either NTN1 of NTN4 dramatically reduces lung bud formation (Liu et al., 2004). Similarly, early vascular development in embryos carrying loss-of-function alleles in *Ntn1* appears normal, even though treatment of vascular smooth muscle cells and endothelial cells with NTN1 stimulates proliferation, induces migration and promotes adhesion of these cells (Park et al., 2003). In our studies, the phenotypes exhibited in glands harboring homozygous deletions of either *Slit2* or *Netrin1* are relatively mild and largely confined to the highly specialized EB (Fig. 3) (Srinivasan et al., 2003). A more dramatic phenotype required deletion of both these guidance cues as they both appear to mediate adhesive, short-range associations between neighboring cell types (Figs 4, 5). Taken together, these results suggest that deciphering the actions of 'axon guidance' cues that function in similar ways (e.g. adhesively during organ development) will require the analysis of compound homozygous null animals to eliminate the expression of more than one member of functionally related families. Future studies in the mammary gland and other organ systems may elucidate other combinations of Netrin, Slit, Semaphorin or Ephrin proteins that function synergistically to mediate cell contacts during development.

We thank the following people for their generous contributions: Pamela Rabbitts for her gift of anti-ROBO1/DUTT1, Santa Cruz Biotech for anti-SLITs, David Garrod for anti- desmosomal constituents, Christelle Sabatier for SLIT2, David Ornitz for *Slit3*$^{-/-}$ mice, and Gary Silberstein and Andrew Chisholm for comments on the manuscript. This work was supported by a research scholar grant #RSG0218001MGO from the American Cancer Society, Career grant DAMD170210336 from the US Army Research Command and research grant 10PB-0188 from the California Breast Cancer Research Program.

Supplementary material

Supplementary material for this article is available at
http://dev.biologists.org/cgi/content/full/133/5/823/DC1

References

Balzar, M., Prins, F. A., Bakker, H. A., Fleuren, G. J., Warnaar, S. O. and Litvinov, S. V. (1999a). The structural analysis of adhesions mediated by Ep-CAM. *Exp. Cell Res.* **246**, 108-121.

Balzar, M., Winter, M. J., de Boer, C. J. and Litvinov, S. V. (1999b). The biology of the 17-1A antigen (Ep-CAM). *J. Mol. Med.* **77**, 699-712.

Bashaw, G. J., Kidd, T., Murray, D., Pawson, T. and Goodman, C. S. (2000). Repulsive axon guidance: Abelson and Enabled play opposing roles downstream of the roundabout receptor. *Cell* **101**, 703-715.

Brisken, C., Kaur, S., Chavarria, T. E., Binart, N., Sutherland, R. L., Weinberg, R. A., Kelly, P. A. and Ormandy, C. J. (1999). Prolactin controls mammary gland development via direct and indirect mechanisms. *Dev. Biol.* **210**, 96-106.

Clark, K., Hammond, E. and Rabbitts, P. (2002). Temporal and spatial expression of two isoforms of the Dutt1/Robo1 gene in mouse development. *FEBS Lett.* **523**, 12-16.

Colamarino, S. A. and Tessier-Lavigne, M. (1995). The axonal chemoattractant netrin-1 is also a chemorepellent for trochlear motor axons. *Cell* **81**, 621-629.

Daniel, C. W., Strickland, P. and Friedmann, Y. (1995). Expression and functional role of E- and P-cadherins in mouse mammary ductal morphogenesis and growth. *Dev. Biol.* **169**, 511-519.

Darcy, K. M., Zangani, D., Lee, P.-P. L. and Ip, M. (2000). *Isolation and Culture of Normal Rat Mammary Epithelial Cells.* New York: Kluwer Academic/Plenum Press.

Deiner, M. S., Kennedy, T. E., Fazeli, A., Serafini, T., Tessier-Lavigne, M. and Sretavan, D. W. (1997). Netrin-1 and DCC mediate axon guidance locally at the optic disc: loss of function leads to optic nerve hypoplasia. *Neuron* **19**, 575-589.

Delehedde, M., Lyon, M., Sergeant, N., Rahmoune, H. and Fernig, D. G. (2001). Proteoglycans: pericellular and cell surface multireceptors that integrate external stimuli in the mammary gland. *J. Mammary Gland Biol. Neoplasia* **6**, 253-273.

Desai, C. J., Garrity, P. A., Keshishian, H., Zipursky, S. L. and Zinn, K. (1999). The Drosophila SH2-SH3 adapter protein Dock is expressed in embryonic axons and facilitates synapse formation by the RP3 motoneuron. *Development* **126**, 1527-1535.

Dulbecco, R., Allen, W. R. and Bowman, M. (1984). Lumen formation and redistribution of inframembranous proteins during differentiation of ducts in the rat mammary gland. *Proc. Natl. Acad. Sci. USA* **81**, 5763-5766.

Englund, C., Steneberg, P., Falileeva, L., Xylourgidis, N. and Samakovlis, C. (2002). Attractive and repulsive functions of Slit are mediated by different receptors in the Drosophila trachea. *Development* **129**, 4941-4951.

Fan, X., Labrador, J. P., Hing, H. and Bashaw, G. J. (2003). Slit stimulation recruits Dock and Pak to the roundabout receptor and increases Rac activity to regulate axon repulsion at the CNS midline. *Neuron* **40**, 113-127.

Garrity, P. A., Rao, Y., Salecker, I., McGlade, J., Pawson, T. and Zipursky, S. L. (1996). *Drosophila* photoreceptor axon guidance and targeting requires the dreadlocks SH2/SH3 adapter protein. *Cell* **85**, 639-650.

Huminiecki, L., Gorn, M., Suchting, S., Poulsom, R. and Bicknell, R. (2002). Magic roundabout is a new member of the roundabout receptor family that is endothelial specific and expressed at sites of active angiogenesis. *Genomics* **79**, 547-552.

Kang, J. S., Yi, M. J., Zhang, W., Feinleib, J. L., Cole, F. and Krauss, R. S. (2004). Netrins and neogenin promote myotube formation. *J. Cell Biol.* **167**, 493-504.

Kappler, J., Franken, S., Junghans, U., Hoffmann, R., Linke, T., Muller, H. W. and Koch, K. W. (2000). Glycosaminoglycan-binding properties and secondary structure of the C-terminus of netrin-1. *Biochem. Biophys. Res. Commun.* **271**, 287-291.

Kennedy, T. E., Serafini, T., de la Torre, J. R. and Tessier-Lavigne, M. (1994). Netrins are diffusible chemotropic factors for commissural axons in the embryonic spinal cord. *Cell* **78**, 425-435.

Kidd, T., Bland, K. S. and Goodman, C. S. (1999). Slit is the midline repellent for the robo receptor in Drosophila. *Cell* **96**, 785-794.

Klinowska, T. C., Soriano, J. V., Edwards, G. M., Oliver, J. M., Valentijn, A. J., Montesano, R. and Streuli, C. H. (1999). Laminin and beta1 integrins are crucial for normal mammary gland development in the mouse. *Dev. Biol.* **215**, 13-32.

Kramer, S. G., Kidd, T., Simpson, J. H. and Goodman, C. S. (2001). Switching repulsion to attraction: changing responses to slit during transition in mesoderm migration. *Science* **292**, 737-740.

Krause, M., Bear, J. E., Loureiro, J. J. and Gertler, F. B. (2002). The Ena/VASP enigma. *J. Cell Sci.* **115**, 4721-4726.

Leighton, P. A., Mitchell, K. J., Goodrich, L. V., Lu, X., Pinson, K., Scherz, P., Skarnes, W. C. and Tessier-Lavigne, M. (2001). Defining brain wiring patterns and mechanisms through gene trapping in mice. *Nature* **410**, 174-179.

Liu, Y., Stein, E., Oliver, T., Li, Y., Brunken, W. J., Koch, M., Tessier-Lavigne, M. and Hogan, B. L. (2004). Novel role for Netrins in regulating epithelial behavior during lung branching morphogenesis. *Curr. Biol.* **14**, 897-905.

Long, H., Sabatier, C., Ma, L., Plump, A., Yuan, W., Ornitz, D. M., Tamada, A., Murakami, F., Goodman, C. S. and Tessier-Lavigne, M. (2004). Conserved roles for Slit and Robo proteins in midline commissural axon guidance. *Neuron* **42**, 213-223.

Nanba, D., Nakanishi, Y. and Hieda, Y. (2001). Changes in adhesive properties of epithelial cells during early morphogenesis of the mammary gland. *Dev. Growth Differ.* **43**, 535-544.

Park, K. W., Morrison, C. M., Sorensen, L. K., Jones, C. A., Rao, Y., Chien, C. B., Wu, J. Y., Urness, L. D. and Li, D. Y. (2003). Robo4 is a vascular-specific receptor that inhibits endothelial migration. *Dev. Biol.* **261**, 251-267.

Plump, A. S., Erskine, L., Sabatier, C., Brose, K., Epstein, C. J., Goodman, C. S., Mason, C. A. and Tessier-Lavigne, M. (2002). Slit1 and Slit2 cooperate to prevent premature midline crossing of retinal axons in the mouse visual system. *Neuron* **33**, 219-232.

Radice, G. L., Ferreira-Cornwell, M. C., Robinson, S. D., Rayburn, H., Chodosh, L. A., Takeichi, M. and Hynes, R. O. (1997). Precocious mammary gland development in P-cadherin-deficient mice. *J. Cell Biol.* **139**, 1025-1032.

Rhee, J., Mahfooz, N. S., Arregui, C., Lilien, J., Balsamo, J. and VanBerkum, M. F. (2002). Activation of the repulsive receptor Roundabout inhibits N-cadherin-mediated cell adhesion. *Nat. Cell. Biol.* **4**, 798-805.

Robinson, G. W., Accili, D. and Hennighausen, L. (2000). Rescue of mammary epithelium of early lethal phenotypes by embryonic mammary gland transplantation as exemplified with insulin receptor null mice. In *Methods in Mammary Gland Biology and Breast Cancer Research* (ed. M. Ip and B. Asch). New York: Kluwer Academic/Plenum Press.

Ronca, F., Andersen, J. S., Paech, V. and Margolis, R. U. (2001). Characterization of Slit protein interactions with glypican-1. *J. Biol. Chem.* **276**, 29141-29147.

Runswick, S. K., O'Hare, M. J., Jones, L., Streuli, C. H. and Garrod, D. R. (2001). Desmosomal adhesion regulates epithelial morphogenesis and cell positioning. *Nat. Cell. Biol.* **3**, 823-830.

Sabatier, C., Plump, A. S., Ma, L., Brose, K., Murakami, F., Lee, E. Y. and

Tessier-Lavigne, M. (2004). The divergent Robo family protein Rig-1 is a negative regulator of Slit responsiveness requried for midline crossing by commissural axons. *Cell* **117**, 157-169.
Serafini, T., Colamarino, S. A., Leonardo, E. D., Wang, H., Beddington, R., Skarnes, W. C. and Tessier-Lavigne, M. (1996). Netrin-1 is required for commissural axon guidance in the developing vertebrate nervous system. *Cell* **87**, 1001-1014.
Silberstein, G. B. (2001). Postnatal mammary gland morphogenesis. *Microsc. Res. Tech.* **52**, 155-162.
Simpson, J. H., Kidd, T., Bland, K. S. and Goodman, C. S. (2000). Short-range and long-range guidance by slit and its Robo receptors. Robo and Robo2 play distinct roles in midline guidance. *Neuron* **28**, 753-766.
Srinivasan, K., Strickland, P., Valdes, A., Shin, G. C. and Hinck, L. (2003). Netrin-1/neogenin interaction stabilizes multipotent progenitor cap cells during mammary gland morphogenesis. *Dev. Cell* **4**, 371-382.
Steigemann, P., Molitor, A., Fellert, S., Jackle, H. and Vorbruggen, G. (2004). Heparan sulfate proteoglycan syndecan promotes axonal and myotube guidance by slit/robo signaling. *Curr. Biol.* **14**, 225-230.
Stein, E. and Tessier-Lavigne, M. (2001). Hierarchical organization of guidance receptors: silencing of netrin attraction by slit through a Robo/DCC receptor complex. *Science* **291**, 1928-1938.
Wang, B., Xiao, Y., Ding, B. B., Zhang, N., Yuan, X., Gui, L., Qian, K. X., Duan, S., Chen, Z., Rao, Y. et al. (2003). Induction of tumor angiogenesis by Slit-Robo signaling and inhibition of cancer growth by blocking Robo activity. *Cancer Cell* **4**, 19-29.
Wang, K. H., Brose, K., Arnott, D., Kidd, T., Goodman, C. S., Henzel, W. and Tessier-Lavigne, M. (1999). Biochemical purification of a mammalian slit protein as a positive regulator of sensory axon elongation and branching. *Cell* **96**, 771-784.
Wong, K., Ren, X. R., Huang, Y. Z., Xie, Y., Liu, G., Saito, H., Tang, H., Wen, L., Brady-Kalnay, S. M., Mei, L. et al. (2001). Signal transduction in neuronal migration: roles of GTPase activating proteins and the small GTPase Cdc42 in the Slit-Robo pathway. *Cell* **107**, 209-221.
Young, L. J. T. (2000). The cleared mammary fat pad and the transplantation of mammary gland morphological structures and cells. New York: Kluwer Academic/Plenum Press.
Yu, T. W., Hao, J. C., Lim, W., Tessier-Lavigne, M. and Bargmann, C. I. (2002). Shared receptors in axon guidance: SAX-3/Robo signals via UNC-34/Enabled and a Netrin-independent UNC-40/DCC function. *Nat. Neurosci.* **5**, 1147-1154.
Zhang, F., Ronca, F., Linhardt, R. J. and Margolis, R. U. (2004). Structural determinants of heparan sulfate interactions with Slit proteins. *Biochem. Biophys. Res. Commun.* **317**, 352-357.